Grid Intersection Graphs and Order Dimension*

Steven Chaplick and Stefan Felsner and
Udo Hoffmann and Veit Wiechert

{chaplick,felsner,uhoffman,wiechert}@math.tu-berlin.de

Institut für Mathematik, Technische Universität Berlin
Straße des 17. Juni 136, D-10623 Berlin, Germany

24. November 2015

We study subclasses of grid intersection graphs from the perspective of order dimension. We show that partial orders of height two whose comparability graph is a grid intersection graph have order dimension at most four. Starting from this observation we provide a comprehensive study of classes of graphs between grid intersection graphs and bipartite permutation graphs and the containment relation on these classes. Order dimension plays a role in many arguments.

1 Introduction

One of the most general standard classes of geometric intersection graphs is the class of *string graphs*, i.e., the intersection graphs of curves in the plane. String graphs were introduced to study electrical networks [26]. The *segment intersection graphs* form a natural subclass of string graphs, where the curves are restricted to straight line segments. We study subclasses where the line segments are restricted to only two different slopes and parallel line segments do not intersect. This class is known as the class of *grid intersection graphs* (GIG). An important feature of this class is that the graphs are bipartite. Subclasses of GIGs appear in several technical applications. For example in *nano PLA-design* [24] and for detecting *loss of heterozygosity events in the human genome* [17].

Other restrictions on the geometry of the representation are used to study algorithmic problems. For example, *stabbability* has been used to study hitting sets and independent sets in families of rectangles [7]. Additionally, computing the jump number of a poset, which is NP-hard in general, has been shown solvable in polynomial time for bipartite posets with interval dimension two using their restricted GIG representation [29].

*Steven Chaplick is supported by ESF EuroGIGA project GraDR, Stefan Felsner is partially supported by DFG grant FE-340/7-2 and ESF EuroGIGA project GraDR , Udo Hoffmann and Veit Wiechert are supported by the Deutsche Forschungsgemeinschaft within the research training group 'Methods for Discrete Structures' (GRK 1408)

Beyond these graph classes that have been motivated by applications and algorithmic considerations, we also study several other natural intermediate graph classes. All these graph classes and properties are formally defined in Subsection 1.1.

The main contribution of this work is to establish the strict containment and incomparability relations depicted in Figure 1. We additionally relate these classes to incidence posets of planar and outerplanar graphs.

In Section 2 we use the geometric representations to establish the containment relations between the graph classes as shown in Figure 1. The maximal dimension of graphs in these classes is the topic of Section 3. In Section 4 we use vertex-edge incidence posets of planar graphs to separate some of these classes from each other. Specifically, we show that the vertex-edge incidence posets of planar graphs are a subclass of *stabbable* GIG (StabGIG), and that vertex-edge incidence posets of outerplanar graphs are a subclass of *stick intersection graphs* (Stick) and *unit* GIG (UGIG). The remaining classes are separated in Section 5. The separating examples are listed in Table 1. As part of this, we show that the vertex-face incidence posets of outerplanar graphs are *segment-ray intersection graphs* (SegRay). As a corollary we obtain that they have interval dimension at most 3.

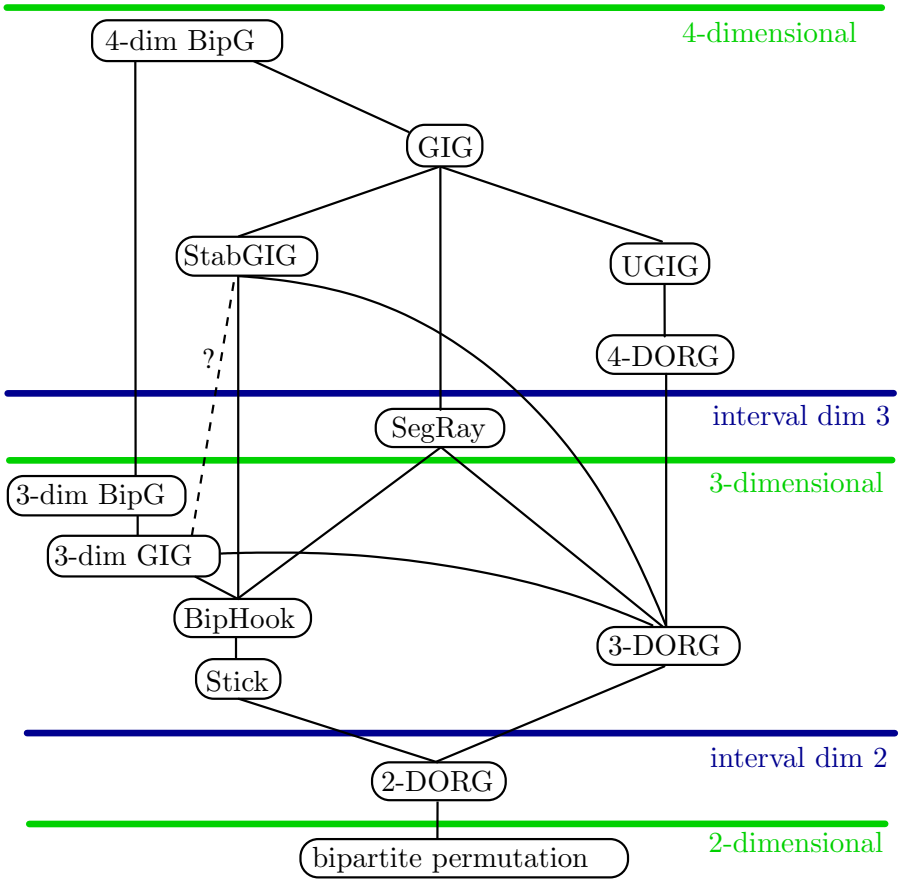

Figure 1: The inclusion order of graph classes studied in this paper.

Class I	$\not\subseteq$	Class II	Example
GIG		3-dim BipG	S_4
3-dim BipG		GIG/3-dim GIG	Proposition 17
3-dim GIG		SegRay	P_{K_4}, Proposition 11
		3-dim BipG	Proposition 17
StabGIG		3-dim GIG	S_4
		SegRay	S_4
SegRay		3-dim GIG	Proposition 16
		StabGIG	Proposition 23
UGIG		3-dim GIG	S_4
		StabGIG	Proposition 24
		4-DORG	C_{14}, see [25]
		SegRay	S_4, Proposition 7
BipHook		3-DORG	Trees
		Stick	Proposition 20
Stick		UGIG	Proposition 18
4-DORG		3-dim GIG	S_4
		StabGIG	Proposition 24
		SegRay	S_4
		3-DORG	S_4
3-DORG		BipHook	Proposition 19
2-DORG		2-dim BipG	S_3

Table 1: Examples separating graph classes in Figure 1

1.1 Definitions of Graph Classes

We introduce the graph classes from Figure 1. A typical drawing of a representation is shown in Figure 2. We denote the class of bipartite graphs by BipG. A *grid intersection graph* (GIG) is an intersection graph of horizontal and vertical segments in the plane where parallel segments do not intersect. Some authors refer to this class as *pure-GIG*. If G admits a grid intersection representation such that all segments have the same length, then G is a *unit grid intersection graph* (UGIG).

A segment s in the plane is *stabbed* by a line ℓ if s and ℓ intersect. A graph G is a *stabbable grid intersection graph* (StabGIG) if it admits a grid intersection representation such that there exists a line that stabs all the segments of the representation. Stabbable representations are generally useful in algorithmic settings as they provide a linear ordering on the objects involved, see [7, 10].

A *hook* is the union of a horizontal and a vertical segment that share the left respectively top endpoint. The common endpoint, i.e., the bend of the hook, is called the *center* of the hook. A graph G is a *hook graph* if it is the intersection graph of a family of hooks whose centers are all on a line ℓ with positive slope (usually ℓ is assumed to be the line $x = y$). Hook graphs have been introduced and studied in [3, 17], [18], and [27]. The graphs are called *max point-tolerance graphs* in [3] and *loss of heterozygosity graphs* in [17]. Typically these graphs are not bipartite. We study the subclass of bipartite hook graphs (BipHook).

A hook graph admitting a representation where every hook is degenerate, i.e., it is a line segment, is a *stick intersection graph* (Stick). In other words, Stick graphs are the

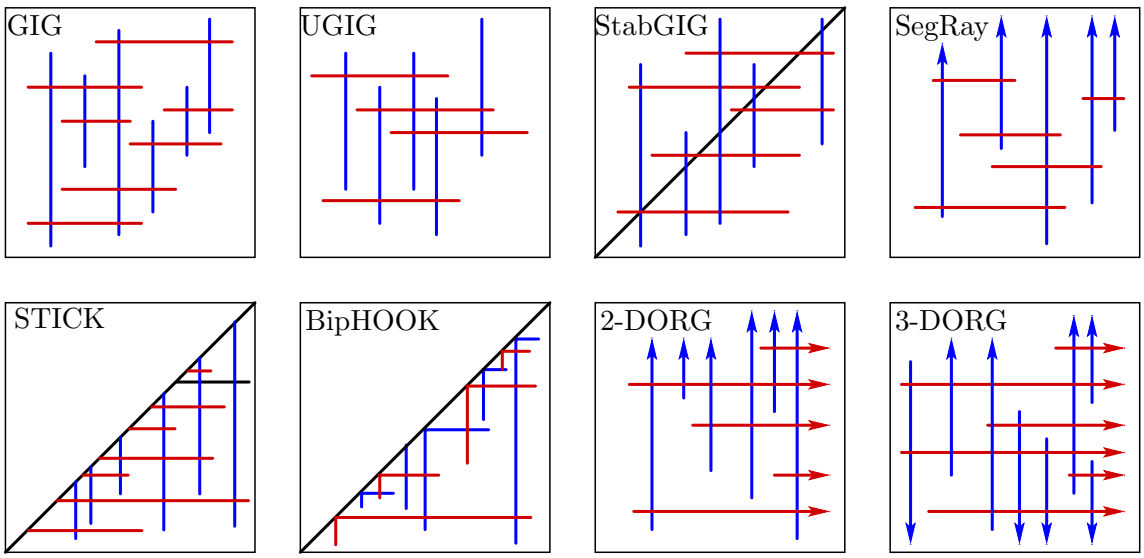

Figure 2: Typical intersection representations of graphs in the graph classes studied in this paper.

intersection graphs of horizontal or vertical segments that have their left respectively top endpoint on a line ℓ with positive slope.

Intersection graphs of rays (or half-lines) in the plane have been previously studied in the context of their chromatic number [20] and the clique problem [2]. We consider some natural bipartite subclasses of this class. Consider a set of axis-aligned rays in the plane. If the rays are restricted into two orthogonal directions, e.g. up and right, their intersection graph is called a *two directional orthogonal ray graph* (2-DORG). This class has been studied in [25] and [29]. Analogously, if three or four directions are allowed for the rays, we talk about 3-DORGs or 4-DORGs. The class of 4-DORGs was introduced in connection with defect tolerance schemes for nano-programmable logic arrays [24].

Finally, segment-ray graphs (SegRay) are the intersection graphs of horizontal segments and vertical rays directed in the same direction. SegRay graphs (and closely related graph classes) have been previously discussed in the context of covering and hitting set problems (see e.g., [19, 4, 5]).

In the representations defining graphs in all these classes we can assume the x and the y-coordinate of endpoints of any two different segments are distinct. This property can be established by appropriate perturbations of the segments.

The *comparability graph* of a poset $P = (X, \leq_P)$ is the graph (X, E) where for distinct $u, v \in X$ we have $uv \in E$ if and only if $u \leq_P v$ or $v \leq_P u$. Every bipartite graph $G = (A, B; E)$ is the comparability graph of a height-2 poset, denoted Q_G, where A is the set of minimal elements, B is the set of maximal elements, and for each $a \in A$, $b \in B$ we have $a \leq b$ in Q_G if and only if a and b are adjacent in G. For the sake of brevity we define the *dimension of a bipartite graph* G to be equal to the dimension of Q_G. The freedom that we may have in defining Q_G, i.e., the choice of the color classes, does not affect the dimension. This is an easy instance of the fact that dimension is a comparability invariant (see [31]).

1.2 Background on order dimension

Let $P = (X, \leq_P)$ be a partial order. A linear order $L = (X, \leq_L)$ on X is a *linear extension* of P when $x \leq_P y$ implies $x \leq_L y$. A family $\mathcal{R}$ of linear extensions of P is a *realizer* of P if $P = \bigcap_{i \in \mathcal{R}} L_i$, i.e., $x \leq_P y$ if and only if $x \leq_L y$ for every $L \in \mathcal{R}$. The *dimension* of P, denoted $\dim(P)$, is the minimum size of a realizer of P. This notion of dimension for partial orders was defined by Dushnik and Miller [11]. The dimension of P can, alternatively, be defined as the minimum t such that P admits an order preserving embedding into the product order on $\mathbb{R}^t$, i.e., we can associate a t-vector $(x_1, \ldots, x_t)$ of reals for each element $x \in X$ such that $x \leq_P y$ if and only if $x_i \leq y_i$ for all $i \in \{1, \ldots, t\}$, which is denoted by $x \leq_{\text{prod}} y$. Trotter's monograph [30] provides a comprehensive collection of topics related to order dimension.

An *interval order* is a partial order $P = (X, <_P)$ admitting an interval representation, i.e., a mapping $x \to (a_x, b_x)$ from the elements of P to intervals in $\mathbb{R}$ such that $x <_P y$ if and only if $b_x \leq a_y$. The *interval dimension* of P, denoted $\text{idim}(P)$, is the minimum number t such that there exist t interval orders I_i with $P = \bigcap_{i=1}^{t} I_i$. Since every linear order is an interval order $\text{idim}(P) \leq \dim(P)$ for all P. If P is of height two, then dimension and interval dimension differ by at most one, i.e., $\dim(P) \leq \text{idim}(P) + 1$, [30, page 47].

Some subclasses of grid intersection graphs are characterised by their order dimension. For example, posets of height 2 and dimension 2 correspond to bipartite *permutation graphs*. Bipartite permutation graphs have an intersection representation of horizontal and vertical segments whose endpoints lie on two parallel lines in the plane: Drawing the first linear extension on a line and the reverse of the second linear extension on a parallel line leads to a segment intersection representation of the permutation graph after connecting the corresponding points on the lines by a segment. In the bipartite case the endpoints can be arranged on the lines such that the segments of the same color class are parallel. Another example of a class of grid intersection graphs which is characterised by a variant of dimension is the class of 2-DORGs.

Proposition 1 *2-DORGs are exactly the bipartite graphs of interval dimension 2.*

This has been shown in [25] using a characterization of 2-DORGs as the complement of co-bipartite circular arc graphs. Below we give a simple direct proof.

To explain it we begin with a geometric version of interval dimension: Vectors $a, b \in \mathbb{R}^d$ with $a \leq_{\text{prod}} b$ define a *standard box* $[a, b] = \{v : a \leq_{\text{prod}} v \leq_{\text{prod}} b\}$ in $\mathbb{R}^d$. Let $P = (X, \leq_P)$ be a poset. A family of standard boxes $\{[a_x, b_x] \subseteq \mathbb{R}^d : x \in X\}$ is a *box representation* of P in $\mathbb{R}^d$ if it holds that $x <_P y$ if and only if $b_x \leq_{\text{prod}} a_y$. Then the interval dimension of P is the minimum d for which there is a box representation of P in $\mathbb{R}^d$. Note that if P has height 2 with $A = \text{Min}(P)$ and $B = \text{Max}(P)$, then in a box representation the lower corner a_x for each $x \in A$ and the upper corner b_y for each $y \in B$ are irrelevant, in the sense that they can uniformly be chosen as $(-c, \ldots, -c)$ respectively $(c, \ldots, c)$ for a large enough constant c.

Proof of Proposition 1. Let $G = (A, B; E)$ be a bipartite graph and suppose $\text{idim}(G) = 2$. Consider a box representation $\{[a_x, b_x]\}$ of G in $\mathbb{R}^2$. Clearly, for each $x \in A$, $y \in B$ we have $xy \in E$ if and only if $b_x \leq_{\text{prod}} a_y$. To obtain a 2-DORG representation of G, draw upward rays starting from upper corners of boxes representing A, and leftward rays starting from lower corners of boxes representing B (see Figure 3). Then for each $x \in A$, $y \in B$ we have $b_x \leq_{\text{prod}} a_y$ if and only if the rays of x and y intersect.

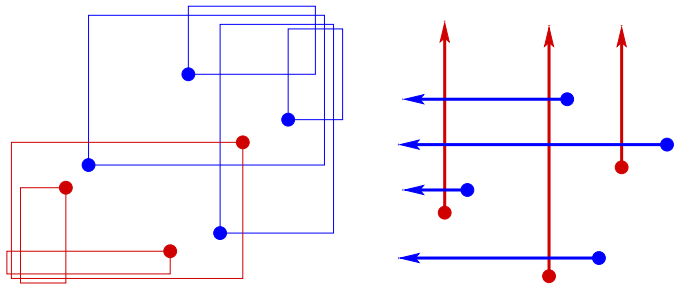

Figure 3: A representation with boxes showing that $\mathrm{idim}(G) = 2$ and the corresponding 2-DORG representation.

Now, the converse direction is immediate together with the observation from the previous paragraph. □

Since the 2-DORGs are exactly the bipartite graphs of interval dimension 2, and interval dimension is bounded by dimension, we obtain

$$\text{2-dim BipG} \subseteq \text{2-DORG}.$$

2 Containment relations between the classes

The diagram shown in Figure 1 has 19 non-transitive inclusions represented by the edges. In this section we show the inclusion between the respective classes of graphs. The inclusion 2-dim BipG $\subseteq$ 2-DORG was already noted as a consequence of Proposition 1. The next 8 inclusions follow directly from the definition of the classes:

$$\begin{array}{cc} \text{UGIG} \subseteq \text{GIG} & \text{StabGIG} \subseteq \text{GIG} \\ \text{2-DORG} \subseteq \text{3-DORG} & \text{3-DORG} \subseteq \text{4-DORG} \\ \text{3-dim GIG} \subseteq \text{3-dim BipG} & \text{3-dim BipG} \subseteq \text{4-dim BipG} \\ \text{Stick} \subseteq \text{BipHook} & \text{3-dim GIG} \subseteq \text{GIG}. \end{array}$$

The following less trivial inclusions follow from geometric modifications of the representation. The proofs are given in the following two propositions.

$$\text{BipHook} \subseteq \text{StabGIG} \qquad \text{2-DORG} \subseteq \text{Stick}.$$

Proposition 2 *Each bipartite hook graph is a stabbable GIG.*

Proof. Let $G = (A, B; E)$ be a bipartite hook graph and fix a hook representation of G in which vertices of A and B are represented by blue and red hooks, respectively. We reflect the horizontal part of each blue hook (dotted in Figure 4) and the vertical part of each red hook (red dotted) at the diagonal. We claim that this results in a StabGIG representation of the same graph. The edges are preserved by the operation, since each intersection is witnessed by a vertical and a horizontal segment, and either both segments are reflected or none of them. On the other hand, the transformation is an invertible linear transformation

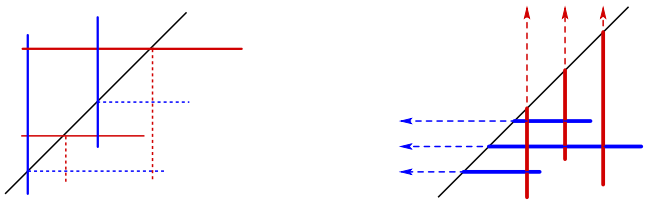

Figure 4: From a BipHook to a StabGIG and from a 2-DORG to a Stick representation.

on a subset of the segments from the region below the line to the one above, hence no new intersection is introduced. The stabbability of the GIG representation comes for free. □

Proposition 3 *Each 2-DORG is a Stick graph.*

Proof. Given a 2-DORG representation of G with upward and leftward rays, we let ℓ be a line with slope 1 that is placed above all intersection points and endpoints of rays. Removing the parts of the rays that lie in the halfplane above ℓ leaves a Stick representation of G, see Figure 4. □

Pruning of rays also yields the following three inclusions:

$$\text{3-DORG} \subseteq \text{SegRay} \qquad \text{SegRay} \subseteq \text{GIG} \qquad \text{4-DORG} \subseteq \text{UGIG}.$$

For the last one, consider a 4-DORG representation and a square of size D that contains all intersections and endpoints of the rays. Cutting each ray to a segment of length D leads to a UGIG representation of the same graph. This was already observed in [25].

Conversely, extending the vertical segments of a Stick representation to vertical upward rays yields:

$$\text{Stick} \subseteq \text{SegRay}.$$

To show that every 3-DORG is a StabGIG, we use a simple geometric argument as depicted in Figure 5 and formalized in the following proposition.

$$\text{3-DORG} \subseteq \text{StabGIG}.$$

Proposition 4 *Each 3-DORG is a stabbable GIG.*

Proof. Consider a 3-DORG representation of a graph G. We assume that vertical rays point up or down while horizontal rays point right. Let s be a vertical line to the right of all the intersections. We prune the horizontal rays at s to make them segments and then reflect the segments at s, this doubles the length of the segments (see Figure 5). Now take all upward rays and move them to the right via a reflection at s. This results in an intersection representation with vertical rays in both directions and horizontal segments such that all rays pointing down are left of s and all rays pointing up are to the right of s. Due to this property we find a line ℓ of positive slope that stabs all the rays and segments of the representation. Pruning the rays above, respectively below their intersection with ℓ yields a StabGIG representation of G. □

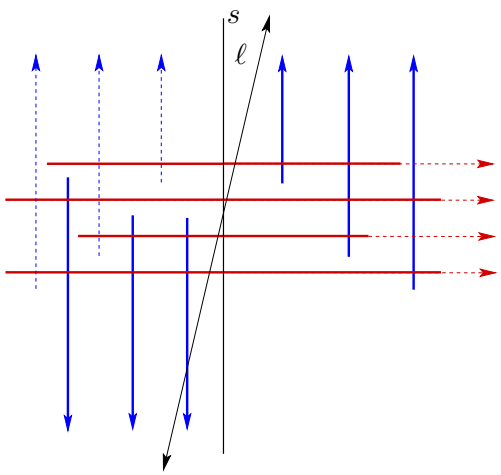

Figure 5: From a 3-DORG to a StabGIG representation

A non-geometric modification of a representation gives the 16^{th} of the 19 non-transitive inclusions from Figure 1:

$$\text{BipHook} \subseteq \text{SegRay}.$$

Proposition 5 *Each bipartite hook graph is a SegRay graph.*

Proof. Consider a BipHook representation of $G = (A, B; E)$. We construct a SegRay representation where A is represented by vertical rays and B by horizontal segments. Let $a_1, \ldots, a_{|A|}$ be the order of the vertices of A that we get by the centers of the hooks on the diagonal, read from bottom-left to top-right. The y-coordinates of the horizontal segments and the endpoints of the rays in our SegRay representation of G will be given in the following way.

We initialize a list $R = [a_1, \ldots, a_{|A|}]$ and a set $S = B$ of *active* vertices, and an empty list Y. We apply one of the following steps repeatedly:

1. If there is an active $a \in R$ such that $N(a) \cap S = \emptyset$, then remove a from R and append it to Y.

2. If there is an active $b \in S$ such that vertices of $N(b)$ appear consecutively in R, then remove b from S and append it to Y.

Suppose that R and S are empty after the iteration. Then we can construct a SegRay representation of G. The endpoint of the ray representing a_i receives i as the x-coordinate and the position of a_i in Y as the y-coordinate. The segment representing $b \in B$ also obtains the y-coordinate according to its position in Y. Its x-coordinates are determined by its neighbourhood. Now it is straight-forward to verify that this defines a SegRay representation of G.

It remains to show that one of the steps can always be applied if R and S are nonempty. Suppose that none of the steps can be applied. Then, for each $b \in S$ there are active vertices $a_i, a_k \in R \cap N(b)$ and $a_j \in R \setminus N(b)$ with $i < j < k$. We call (a_j, b) an *interesting pair*. If

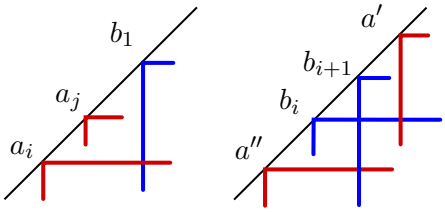

Figure 6: Left: b_1 is not involved in a forward pair. Right: A forbidden configuration for a bipartite hook graph.

the center of the hook a_j lies before the center of b then we call the interesting pair *forward*, and *backward* otherwise. Let $b_1, \ldots, b_{|S|}$ be the order of centers of active vertices of S. If b_1 is involved in a forward interesting pair, then each certifying a_j is locked in the triangle between b_1 and a_i and thus has no neighbour in S (see Figure 6), and so step 1 could be applied. Hence every interesting pair involving b_1 is a backward pair. Symmetrically, every interesting pair involving $b_{|s|}$ is a forward pair. We conclude that there are active vertices b_i, b_{i+1}, such that b_i is involved in a forward interesting pair, and b_{i+1} in a backward one.

Let $a' \in N(b_i)$ be the hook corresponding to an active vertex that encloses $a \notin N(b_i)$, i.e., $b_i < a < a'$ on the diagonal. Since a is active its hook intersects some b_j with $i+1 \leq j$. Therefore, $b_i < b_{i+1} < a'$ on the diagonal. By symmetric reasoning we also find $a'' \in N(b_{i+1})$ such that on the diagonal $a'' < b_i < b_{i+1} < a'$ and $a''b_{i+1} \in E$. The order on the diagonal and the existence of edges $a''b_{i+1}$ and b_ia' implies that the hooks of b_i and b_{i+1} intersect (see Figure 6). This contradicts that b_i and b_{i+1} belong to the same color class of the bipartite graph. □

3 Dimension

From the 19 inclusion relations between classes that have been mentioned at the beginning of the previous section we have shown 16. The remaining three inclusions will be shown by using order dimension in this section. Specifically, we bound the maximal dimension of the graphs in the relevant classes. First, we will show that the dimension of GIGs is bounded. It has previously been observed that $\text{idim}(G) \leq 4$ when G is a GIG [6]. As already shown in [13] this can be strengthened to $\dim(G) \leq 4$.

We define four linear extensions of G as depicted in Figure 7. In each of the directions left, right, top and bottom we consider the orthogonal projection of the segments onto a directed horizontal or vertical line. In each such projection every segment corresponds to one interval (or point) per line. We choose a point from each interval on the line by the following rule. For minimal elements we take the minimal point in the interval in the direction of the line, for maximal elements we choose the maximal one. We denote those total orders according to the direction of their oriented line by $L_\leftarrow, L_\rightarrow, L_\uparrow, L_\downarrow$.

Proposition 6 *For every GIG G, $\{L_\leftarrow, L_\rightarrow, L_\uparrow, L_\downarrow\}$ is a realizer of G. Hence* $\dim(G) \leq 4$.

Proof. For two intersecting segments the minimum always lies before the maximum, see Figure 7. It remains to check that every incomparable pair (s_1, s_2) is reversed in the realizer.

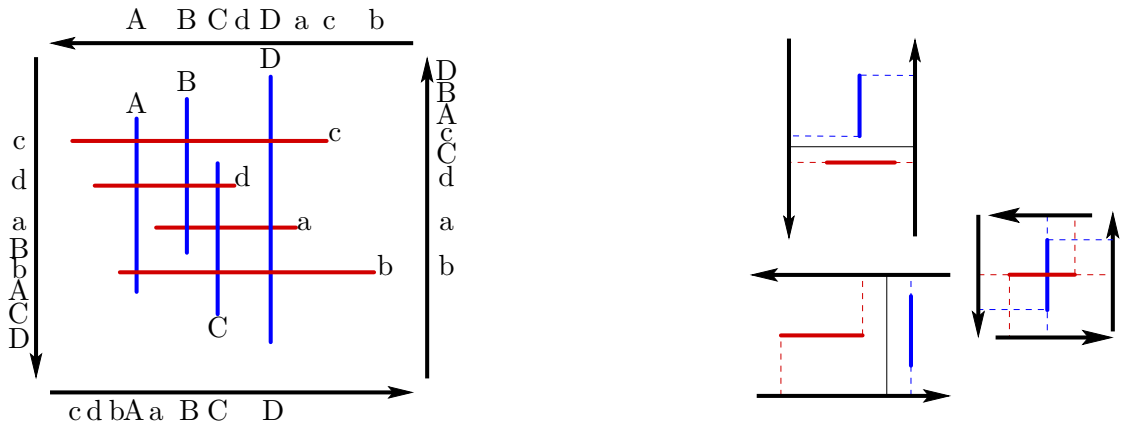

Figure 7: A realizer of a GIG and an illustration of the correctness.

Every disjoint pair of segments is separated by a horizontal or vertical line. The separated vertices appear in different order in the two directions orthogonal to this line, see Figure 7. □

It is known that a bipartite graph is a bipartite permutation graph if and only if the dimension of the poset is at most 2. Thus, by Proposition 6, the maximal dimension of the graphs in the other classes that we consider must be 3 or 4. In the following we show that BipHooks and 3-DORGs have dimension at most 3. For these results we note that graphs with a special SegRay representation have dimension at most 3 and that the interval dimension of SegRay graphs is bounded by 3. This latter result was shown previously by a different argument in [6].

Lemma 1 *For a SegRay graph G, $\dim(G) \leq 3$ when G has a SegRay representation satisfying the following: whenever two horizontal segments are such that the x-projection of one is included in the other one, then the smaller segment lies below the bigger one.*

Proof. Consider such a SegRay representation of G with horizontal segments as maximal and downward rays as minimal elements of Q_G. The linear extensions $L_{\rightarrow}$, $L_{\leftarrow}$, and $L_{\downarrow}$ defined for Proposition 6 form a realizer of Q_G. □

Corollary 1 *For every 3-DORG G, $\dim(G) \leq 3$.*

Proof. Consider a 3-DORG representation of G where the horizontal rays use two directions. We cut the horizontal rays so that they have the same length D. When D is large enough, this yields a SegRay representation of the same graph. Note that such a representation has no nested segments. Thus, Lemma 1 implies $dim(Q_G) \leq 3$. □

Proposition 7 *For every SegRay graph G, $\mathrm{idim}(G) \leq 3$.*

Proof. Suppose that the rays correspond to minimal elements of Q_G. By Lemma 1 the linear extensions $L_{\rightarrow}$, $L_{\leftarrow}$ and $L_{\downarrow}$ reverse all incomparable pairs except some that consist

of two maximal elements. We convert these linear extensions to interval orders and extend the intervals (originally points) of maximal elements in $L_{\rightarrow}$ far to the right to make them intersect. In this way we obtain three interval orders whose intersection gives rise to Q_G. □

Proposition 8 *For every bipartite hook graph G, $\dim(G) \leq 3$.*

Proof. Let A and B be the color classes of G. We construct the graph G' by adding private neighbours to vertices of B. Then G' is also a BipHook graph as we can easily add hooks intersecting a single hook in a representation of G. By Proposition 5 we know that G' has a SegRay representation R with downward rays representing A. By construction, each horizontal segment in R must have its private ray intersecting it. Thus R satisfies the property of Lemma 1 and $\dim(Q_{G'}) \leq 3$. Since Q_G is an induced subposet of $Q_{G'}$ we conclude $\dim(Q_G) \leq 3$. □

Since Stick $\subset$ BipHook we know that $\dim(Q_G) \leq 3$ if G is a Stick graph. However, a nicer realizer for a Stick graph is obtained by Proposition 6, since $L_{\leftarrow}$ and $L_{\downarrow}$ coincide in a Stick representation.

In Section 5 we will show that these bounds are tight.

4 Vertex-Edge Incidence Posets

We proceed by investigating the relations between the classes of GIGs and incidence posets of graphs.

For a graph G, P_G denotes the vertex-edge incidence poset of G, and the comparability graph of P_G is the graph obtained by subdividing each edge of G once. The vertex-edge incidence posets of dimension 3 are characterised by Schnyder's Theorem.

Theorem 1 ([23]) *A graph G is planar if and only if $\dim(P_G) \leq 3$.*

Even though some GIGs have poset dimension 4, we will see that the vertex-edge incidence posets with a GIG representation are precisely the vertex-edge incidence posets of planar graphs.

A *weak bar-visibility representation* of a graph is a drawing that represents the vertices as horizontal segments and the edges as vertical segments (sight lines) touching its adjacent vertices.

Theorem 2 ([28, 32]) *A graph G has a weak bar-visibility representation if and only if G is planar.*

A weak bar-visibility representation of G gives a GIG representation of P_G. On the other hand, a GIG representation of P_G can be transformed into a weak bar-visibility representation of G. In particular, since the segments representing edges of G intersect two segments representing incident vertices, they can be shortened until their intersections become contacts. Hence P_G is a GIG if and only if G is planar. We next show the stronger result, that there is a StabGIG representation of P_G for every planar graph G.

Proposition 9 *A graph G is planar if and only if P_G is a stabbable GIG.*

We use the following definitions. A *generic floorplan* is a partition of a rectangle into a finite set of interiorly disjoint rectangles that have no point where four rectangles meet. Two floorplans are *weakly equivalent* if there exist bijections Φ_H between the horizontal segments and Φ_V between the vertical segments, such that a segment s has an endpoint on t in F if and only if $\Phi(s)$ has an endpoint on $\Phi(t)$. A floorplan F *covers* a set of points P if and only if every segment contains exactly one point of P and no point is contained in two segments. The following theorem has been conjectured by Ackerman, Barequet and Pinter [1], who have also shown it for the special case of *separable* permutations. It has been shown by Felsner [12] for general permutations.

Theorem 3 ([12]) *Let P be a set of n points in the plane, such that no two points have the same x- or y-coordinate and F a generic floorplan with n segments. Then there exists a floorplan F', such that F and F' are weakly equivalent and F' covers P.*

Proof of Proposition 9. Consider a weak bar-visibility representation of G. The lowest and highest horizontal segments h_b and h_t can be extended, such that their left as well as their right endpoints can be connected by new vertical segments v_l and v_r. The segments h_b, h_t, v_l and v_r are the boundary of a rectangle. Extending every horizontal segment until its left and right endpoints touch vertical segments leads to a floorplan F. By Theorem 3 there exists an equivalent floorplan F' that covers a pointset P consisting of n points on the diagonal of the the big rectangle with positive slope. Shortening the horizontal segments and extending the vertical segments of F' by $\epsilon > 0$ on each end leads to a GIG representation of P_G that can be stabbed by the line through the diagonal.

On the other hand, every GIG representation of P_G leads to a weak bar-visibility representation, and hence G is planar. □

We will now show that P_G is in the classes of Stick and bipartite hook graphs if and only if G is outerplanar.

Proposition 10 *P_G is a Stick graph if and only if G is outerplanar.*

Proof. Outerplanar graphs have been characterized by linear orderings of their vertices by Felsner and Trotter [16]: A graph $G = (V, E)$ is outerplanar if and only if there exist linear orders L_1, L_2, L_3 of the vertices with $L_2 = \overleftarrow{L_1}$, i.e., L_2 is the reverse of L_1, such that for each edge $vw \in E$ and each vertex $u \notin \{v, w\}$ there is $i \in \{1, 2, 3\}$, such that $u > v$ and $u > w$ in L_i.

Consider a Stick representation of P_G where the elements of V correspond to vertical sticks. Restricting the linear extensions $L_1 = L_{\leftarrow}$, $L_2 = L_{\rightarrow}$, and $L_3 = L_{\uparrow}$ (cf. the proof of Proposition 6) obtained from a Stick representation of P_G to the elements of V yields linear orders satisfying the property above. Thus G is outerplanar.

For the backward direction let G be an outerplanar graph. In [3] it is shown that the class of *hook contact* graphs (each intersection of hooks is also an endpoint of a hook) is exactly the class of outerplanar graphs. Given a hook contact representation of G we construct a Stick representation of P_G. To this end we consider each hook as two sticks, a vertical one for the vertices and a horizontal one as a placeholder for the edges. For each contact of the

horizontal part of a hook v we place an additional horizontal stick slightly below the center of v. The k-th contact of a hook with the horizontal part is realized by the k-th highest edge that is added in the placeholder as shown in Figure 8. □

Figure 8: A hook contact representation of G transformed into a Stick representation of P_G.

We continue by providing some characterizations of outerplanar graphs according to GIG representations of vertex-edge incidence posets.

A *weak semibar-visibility representation* of a graph is a drawing that represents the vertices as vertical segments with lower end at the horizontal line $y = 0$, and the edges as horizontal segments touching the two vertical segments that represent incident vertices.

Lemma 2 ([8]) *A graph G is outerplanar if and only if G has a weak semibar-visibility representation.*

The construction used in the previous proposition directly produces a weak semibar-visibility representation of an outerplanar graph. Just extend all vertical segments upwards until they hit a common horizontal line ℓ and reflect the plane at ℓ, now ℓ can play the role of the x-axis for the weak semibar-visibility representation.

Proposition 11 *A graph G is outerplanar if and only if the graph P_G has a SegRay representation where the vertices of G are represented as rays.*

Proof. Cutting the rays of a SegRay representation with rays pointing downwards somewhere below all horizontal segments leads to a weak semibar-visibility representation of G and vice versa. Thus, Lemma 2 gives the result. □

Proposition 12 *A graph G is outerplanar if and only if the graph P_G has a hook representation.*

Proof. If G is outerplanar then P_G has a hook representation by Proposition 10. On the other hand, assume that P_G has a hook representation for a graph G. According to Proposition 5 we construct a SegRay representation with vertices as rays and edges as segments. This representation shows that G is outerplanar by Proposition 11. □

Proposition 13 *If G is outerplanar, then the graph P_G has a SegRay representation where the vertices of G are represented as segments.*

Proof. Consider a hook representation R' of P_G. According to the proof Proposition 5 we can transform P_G into a SegRay representation with a free choice of the colorclass that is represented by rays. Choosing the subdivision vertices as rays leads to the required representation. □

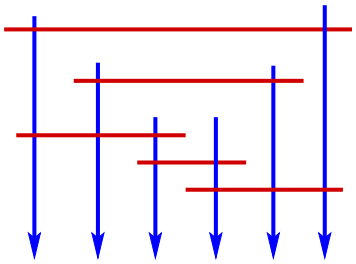

Figure 9: A SegRay representation of $P_{K_{2,3}}$.

In contrast to Proposition 11, the backward direction of Proposition 13 does not hold: Figure 9 shows a SegRay representation of $P_{K_{2,3}}$ with vertices being represented as horizontal segments, but $K_{2,3}$ is not outerplanar. Together with Proposition 11 this also shows that the class of SegRay graphs is not symmetric in its color classes.

In the following we construct a UGIG representation of P_G for an outerplanar graph G.

Proposition 14 *If G is outerplanar then P_G is a UGIG.*

Proof. We construct a UGIG representation of P_G for a maximal outerplanar graph $G = (V, E)$ with outer-face cycle $v_0, \ldots, v_n$. The vertices of V are drawn as vertical segments. Starting from v_0 we iteratively draw the vertices of breadth-first-search layers (BFS-layers). Each BFS-layer has a natural order inherited from the order on the outer-face, i.e., the increasing order of indices. When the i-th layer L_i has been drawn the following invariants hold:

1. Segments for all vertices and edges of $G[L_0, \ldots, L_{i-1}]$, all vertices of L_i, and all edges connecting vertices of L_{i-1} to vertices of L_i have been placed.

2. The upper endpoints of the segments representing vertices in L_i lie on a strict monotonically decreasing curve C_i. Their order on C_i agrees with the order of the corresponding vertices in L_i. Their x-coordinates differ by at most one.

3. No segment intersects the region above C_i.

We start the construction with the vertical segment corresponding to v_0. The curve C_0 is chosen as a line with negative slope that intersects the upper endpoint of v_0.

We start the $(i+1)$-th step by adding segments for the edges within vertices of layer L_i. Afterwards we add the segments for edges between vertices in layer L_i and L_{i+1} and the segments for the vertices of layer L_{i+1}. The construction is indicated in Figure 10.

First we draw unit segments for the edges within layer L_i. Since the graph is outerplanar such edges only occur between consecutive vertices of the layer. For a vertex v_k of L_i which is not the first vertex of L_i we define a horizontal ray r_k whose start is on the segment of

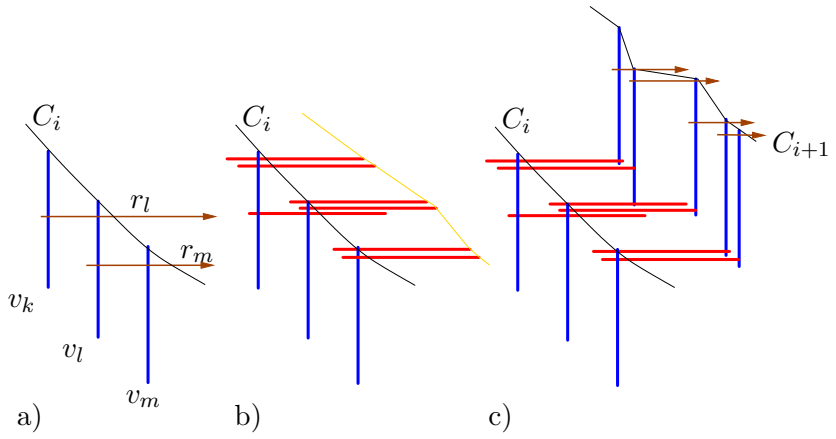

Figure 10: One step in the construction of a UGIG representation of P_G: a)The situation before the step. b) The edges between layer L_i and L_{i+1} and within layer L_i are added. c) The vertices of layer L_{i+1} are added.

the predecessor of v_k on this layer such that the only additional intersection of r_k is with the segment of v_k. The initial unit segment of ray r_k can be used for the edge between v_k and its predecessor.

All segments that will represent edges between layer L_i and L_{i+1} are placed as horizontal segments that intersect the segment of the incident vertex $v_k \in L_i$ above the ray r_k. We draw these edge-segments such that the endpoints lie on a monotonically decreasing curve C and the order of these endpoints on C corresponds to the order of their incident vertices in L_{i+1}.

Now the right endpoints of the edges between the two layers lie on the monotone curve C and no segment intersects the region above this curve. Due to properties of the BFS for outerplanar graphs, each vertex of layer L_{i+1} is incident to one or two edges whose segments end on C and if there are two then they are consecutive on C. We place the unit segments of vertices of L_{i+1}, such that their lower endpoint is on the lower segment of an incident edge with the x-coordinate such that they realize the required intersections.

With this construction the invariants are satisfied. □

There are graphs G where P_G is a UGIG and G is not outerplanar, for example $G = K_{2,3}$ as shown in Figure 11. On the other hand there exist planar graphs G, such that P_G is not a UGIG as the following proposition shows.

Proposition 15 *P_{K_4} is not a UGIG.*

Proof. Suppose to the contrary that P_{K_4} has a UGIG representation with vertices as vertical segments. By contracting vertical segments to points one can obtain a planar embedding of K_4 from such a representation. As K_4 is not outerplanar, there is a vertex v that is not incident to the outer face in this embedding. For the initial UGIG representation this means that v is represented by a vertical segment which is enclosed by segments representing vertices and edges of $K_4 - \{v\}$. Notice that these segments represent a 6-cycle of P_{K_4}. However, the largest vertical distance between any pair of horizontal segments in this cycle

is less than 1. Thus, there is not enough space for the vertical segment of v, contradiction. □

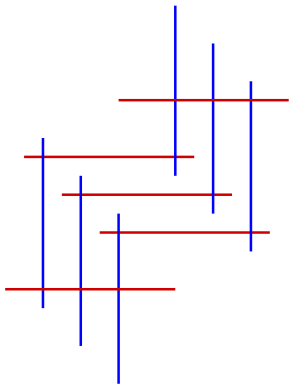

Figure 11: A UGIG representation of $P_{K_{2,3}}$.

5 Separating examples

In this section we will give examples of graphs that separate the graph classes in Figure 1. For this purpose we will show that the classes we have observed to be at most 4-dimensional indeed contain 4-dimensional graphs. This is done in Subsection 5.1 using standard examples and vertex-face incidence posets of outerplanar graphs. The remaining graph classes will be separated using explicit constructions in Subsection 5.2 and Subsection 5.3.

Using the observations of Section 4 about vertex-edge incidence posets we can immediately separate the following graph classes.

$$\text{StabGIG} \not\subset \text{BipHook} \qquad \text{StabGIG} \not\subset \text{3-DORG}$$
$$\text{SegRay} \not\subset \text{4-DORG} \qquad \text{Stick} \not\subset \text{2-DORG}.$$

In [25] it is shown that the graph C_{14} (cycle on 14 vertices) is not a 4-DORG, and in particular is not a 3- or 2-DORG. In other words, P_{C_7} is not a 4-DORG. Since C_7 is outerplanar, by the propositions of the previous section we know that P_{C_7} is a SegRay, a StabGIG and a Stick graph. This shows the three seperations involving DORGs. For the first one let G be a planar graph that is not outerplanar. Then P_G is a StabGIG (Proposition 9) but not a BipHook graph (Proposition 12).

5.1 4-Dimensional Graphs

First of all, some graph classes are already separated by their maximal dimension. The *standard example* S_n of an n-dimensional poset, cf. [30], is the poset on n minimal elements $a_1, \ldots, a_n$ and n maximal elements $b_1, \ldots, b_n$, such that $a_i < b_j$ in S_n if and only if $i \neq j$. To separate most of the 4-dimensional classes from the 3-dimensional ones, the standard example S_4 is sufficient. As shown in Figure 12 it has as a stabbable 4-DORG representation.

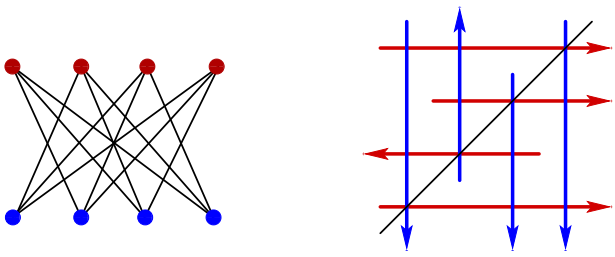

Figure 12: The poset S_4 and a stabbable 4-DORG representation of it.

From this it follows that:

$$\text{StabGIG} \not\subset \text{BipHook} \qquad \text{StabGIG} \not\subset \text{3-DORG}$$
$$\text{4-DORG} \not\subset \text{3-DORG} \qquad \text{StabGIG} \not\subset \text{3-dim GIG}$$

Since the interval dimension of S_n is n we get the following relations from Proposition 7.

$$\text{StabGIG} \not\subset \text{SegRay} \qquad \text{4-DORG} \not\subset \text{SegRay}$$

We will now show that the vertex-face incidence poset of an outerplanar graph has a SegRay representation. In [15] it has been shown that there are outerplanar maps with a vertex-face incidence poset of dimension 4. Together with Proposition 16 below this shows that there are SegRay graphs of dimension 4. We obtain

$$\text{SegRay} \not\subset \text{3-dim GIG}.$$

Proposition 16 *If G is an outerplanar map then the vertex-face incidence poset of G is a SegRay graph.*

Let G be a graph with a fixed outerplanar embedding. First we argue that we may assume that G is 2-connected. If G is not connected then we can add a single edge between two components without changing the vertex-face poset. Now consider adding an edge between two neighbours of a cut vertex on the outer face cycle, i.e., two vertices of distance 2 on this cycle. This adds a new face to the vertex-face-poset, but keeps the old vertex-face-poset as an induced subposet. Therefore, we may assume that G is 2-connected.

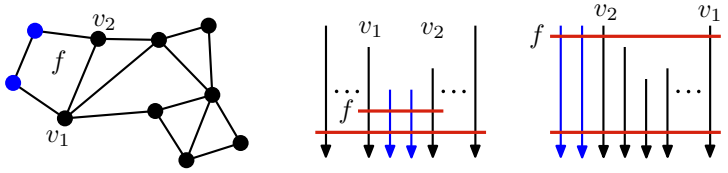

Figure 13: Illustration for the induction step in Proposition 16

By induction on the number of bounded faces we show that G has a SegRay representation in which the cyclic order of the vertices on the outer face agrees with the left-right order (cyclically) of rays representing these vertices. If G has one bounded face then the claim is

straight-forward. If G has more bounded faces then consider the dual graph of G without the outer face, which is a tree. Let f be a face that corresponds to a leaf of that tree. Define G' to be the plane graph obtained by removing f and incident degree-2 vertices from G. Then exactly two vertices v_1, v_2 of f are still in G', and they are adjacent via an edge at the outer face of G'. Note that G' is 2-connected. Applying induction on G' we obtain a SegRay representation in which the two rays representing v_1 and v_2 are either consecutive, or left- and rightmost ray.

In the first case we insert rays for the removed vertices between v_1 and v_2 with endpoints being below all other horizontal segments. Then a segment representing f can easily be added to obtain a SegRay representation with the required properties of G, see the middle of Figure 13.

If the rays of v_1 and v_2 are the left- and rightmost ones, then observe that the endpoints of both rays can be extended upwards to be above all other endpoints. We can insert the new rays to the left of all the other rays and the segment for f as indicated in Figure 13 on the right. This concludes the proof. □

Propositions 16 and 7 also give the following interesting result about vertex-face incidence posets of outerplanar maps which complements the fact that they can have dimension 4 [15].

Corollary 2 *The interval dimension of a vertex-face incidence poset of an outerplanar map is bounded by* 3.

We have separated all the graph classes which involve dimension except for the two classes of 3-dimensional GIGs and stabbable GIGs. As indicated in Figure 1 it remains open whether 3-dim GIG is a subclass of StabGIG or not. More comments on this can be found at the end of Subsection 5.3.

5.2 Constructions

In this subsection we give explicit constructions for the remaining separations of classes not involving StabGIG.

In the introduction we mentioned that every 2-dimensional order of height 2, i.e., every bipartite permutation graph, is a GIG. We show now that this does not hold for 3-dimensional orders of height 2.

Proposition 17 *There is a 3-dimensional bipartite graph that is not a GIG.*

Proof. The left drawing in Figure 14 defines a poset P by ordering the homothetic triangles by inclusion. Some of the triangles are so small that we refer to them as points from now on. Each inclusion in P is witnessed by a point and a triangle, and hence P has height 2. To see that it is 3-dimensional we use the drawing and the three directions depicted in Figure 14. By applying the same method as we did for Proposition 6 we obtain three linear extensions forming a realizer of P.

We claim that P is not a pseudosegment intersection graph[1], and hence not a GIG. Suppose to the contrary that it has a pseudosegment representation. The six green triangles together with the three green and the three blue points form a cycle of length 12 in G.

[1]The intersection graph of curves where each pair of curves intersects in at most one point.

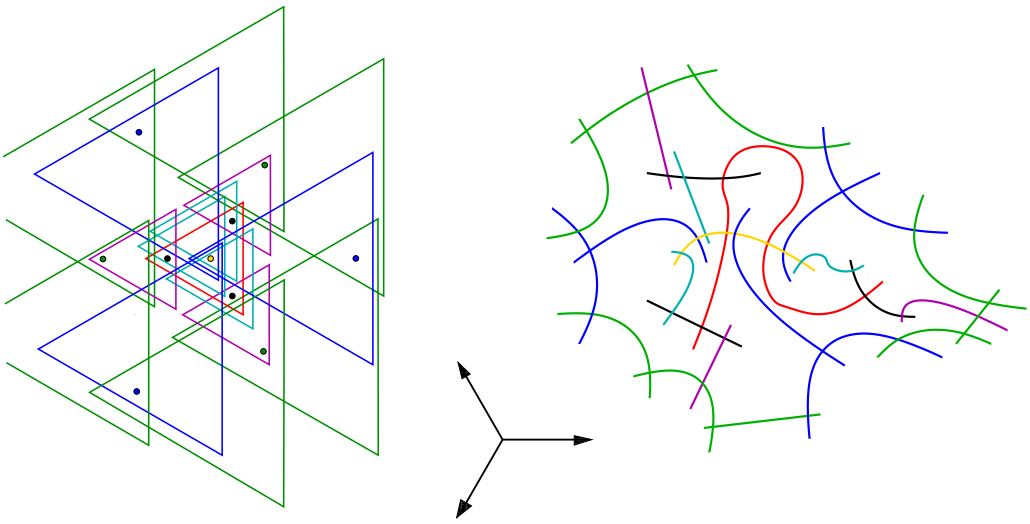

Figure 14: The drawing on the left defines an inclusion order of homothetic triangles. This height-2 order does not have a pseudosegment representation.

Hence, the union of the corresponding pseudosegments in the representation contains a closed curve in $\mathbb{R}^2$. Without loss of generality assume that the pseudosegment representing the yellow point lies inside this closed curve (we may change the outer face using a stereographic projection). The pseudosegments of the three large blue triangles intersect the yellow pseudosegment and one blue pseudosegment (corresponding to a blue point) each. The yellow and the blue pseudosegments divide the interior of the closed curve into three regions. We show that each of these regions contains one of the pseudosegments representing black points.

Each purple pseudosegment intersects the cycle in a point that is incident to one of the three bounded regions. Now, each black pseudosegment intersects a purple one. If such an intersection lies in the unbounded region, then the whole black pseudosegment is contained in this region. This is not possible as for each of the black pseudosegments there is a blue pseudosegment representing a small blue triangle that connects it to the enclosed yellow pseudosegment without intersecting the cycle. Thus, the three intersections of purple and black pseudosegments have to occur in the bounded regions, and in each of them one. It follows that each of the three bounded regions contains one black pseudosegment.

Now, the red pseudosegment intersects each of the three black pseudosegments. Since they lie in three different regions whose boundary it may only traverse through the yellow pseudosegment, it has to intersect the yellow pseudosegment twice. This contradicts the existence of a pseudosegment representation. □

In the following we give constructions to show that

Stick $\not\subset$ UGIG	UGIG $\not\subset$ Stick
BipHook $\not\subset$ 3-DORG	BipHook $\not\subset$ Stick

Proposition 18 *The Stick graph shown in Figure 15 is not a UGIG.*

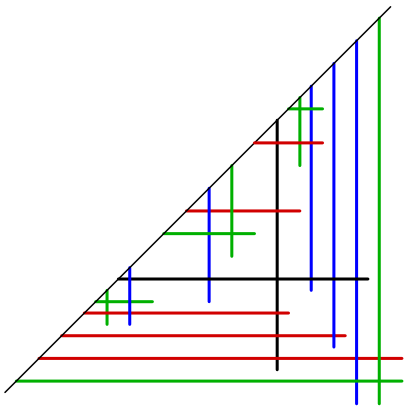

Figure 15: A stick representation of a graph that is not a UGIG.

Proof. Let G be the graph represented in Figure 15. Let v and h be the two adjacent vertices of G that are drawn as black sticks in the figure. There are five pairs of intersecting blue vertical and red horizontal segments $v_1, h_1, \ldots, v_5, h_5$. Each v_i intersects h and each h_i intersects v. Four of the pairs v_i, h_i form a 4-cycle with a pair of green segments q_i, r_i.

Suppose that G has a UGIG representation. We claim that in any such representation the intersection points p_i of v_i and h_i form a chain in $<_{\text{prod}}$ after a suitable rotation of the representation. Note that one quadrant formed by the segments v and h (without loss of generality the upper right one) contains at least two of the p_i's by the pigeonhole principle. Assume without loss of generality that p_1 and p_2 lie in this quadrant. If p_1 and p_2 are incomparable in $<_{\text{prod}}$, then the horizontal segment h_1 of the lower intersection point has a forbidden intersection with the vertical segment v_2 of the higher one, see Figure 16 left.

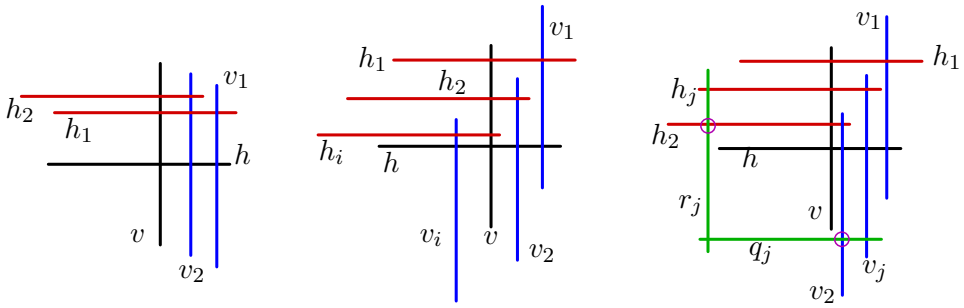

Figure 16: Left: The intersection points p_1, p_2 in the upper right quadrant form a chain in $<_{\text{prod}}$. Middle: p_i does not dominate p_2 in $<_{\text{prod}}$. Right: The green segments q_j, r_j for the middle pair of segments h_j, v_j cannot be added.

So p_1 and p_2 are comparable in $<_{\text{prod}}$. We may assume that v_2, h_2 is the pair of segments whose intersection point is dominated in $<_{\text{prod}}$ by all other intersection points in the upper right quadrant. We observe that the lower endpoint of v_2 lies below the lower endpoint of v, and the left endpoint of h_2 lies to the left of the left endpoint of h as shown in the middle of Figure 16. It follows that if an intersection point p_i does not dominate p_2, then p_i lies below h_2 and to the left of v_2, but not in the upper right quadrant by our choice of p_2 (see Figure 16 for an example). It is easy to see that the remaining two intersection points

p_j ($j \notin \{1, 2, i\}$) then have to dominate p_2 in $<_{\text{prod}}$, as otherwise we would see forbidden intersections among the blue and red segments.

We conclude that, in each case, four of the points $p_1, \ldots, p_5$ lie in the upper right quadrant and that they form a chain with respect to $<_{\text{prod}}$. Thus at least one pair of segments v_j, h_j with p_j being in the middle of the chain has neighbours q_j, r_j. However, as indicated in the right of Figure 16, q_j and r_j cannot be added without introducing forbidden intersections. Hence G does not have a UGIG representation. □

We now show that there is a 3-DORG that is not a BipHook graph. We will use the following lemma for the argument.

Lemma 3 *Let G be a bipartite graph and G' be the graph obtained by adding a twin to each vertex of G (i.e., a vertex with the same neighbourhood). Then G' is a hook graph if and only if G is a Stick graph.*

Proof. Suppose that G' has a hook representation. Consider twins $v, v' \in V(G)$ and the position of their neighbours in a hook representation. Suppose that there are vertices $u, w \in N(v)$, such that the order on the diagonal is u, v, v', w. One can see that this order of centres together with edges uw and $v'u$ would force the hooks of v and v' to intersect, which contradicts their non-adjacency. Thus either no neighbour of v occurs before v or no neighbour of v' occurs after v' on the diagonal. This shows that the hook of v or v' can be drawn as a stick, and it follows that G has a Stick representation.

Conversely, in a stick representation of G twins can easily be added to obtain a stick representation of G'. □

Proposition 19 *The* 3-DORG *in Figure 17 is not a Stick graph.*

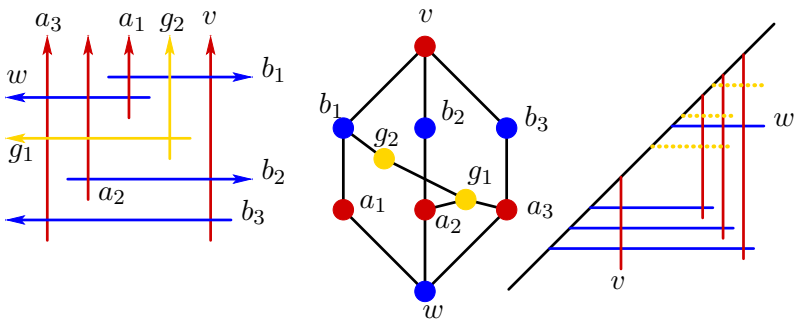

Figure 17: A 3-DORG that is not a Stick graph.

Proof. Suppose to the contrary that a Stick representation of the graph exists. We may assume that v is a vertical and w a horizontal stick. Observe that w has to lie above v on the diagonal: Otherwise, two of the a_i's have to lie either before v or after v, however, for the outer one of such a pair of a_i's it is impossible to place a stick for b_i that also intersects v. Hence, the Stick representation of v, w and the a_i's and b_i's have to look as in Figure 17. By checking all possible positions of g_1, i.e., permutations of $\{a_1, a_2, a_3\}$ and the correspondingly forced permutation of $\{b_1, b_2, b_3\}$ in the representation, it can be verified

that the representation cannot be extended to a representation of the whole graph. The cases are indicated in Figure 17. □

As a consequence, there is a 3-DORG that is not a bipartite hook graph. Indeed, if we add a twin to each vertex of the graph shown in Figure 17 then the obtained graph is still a 3-DORG. It can not be a BipHook graph as otherwise by Lemma 3 we would conclude that the graph in Figure 17 is a Stick graph.

We next show a construction of a bipartite hook graph that is not a Stick graph. A related construction was also presented in [18].

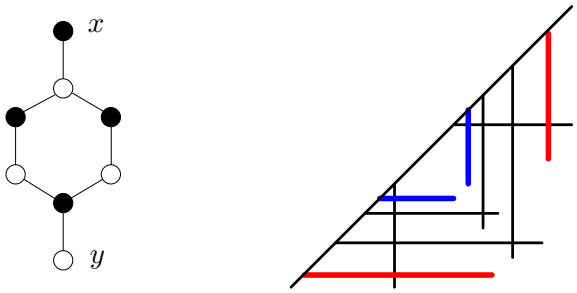

Figure 18: The graph Φ and the two possible positions of x and y in a Stick representation of G.

Proposition 20 *There is a bipartite hook graph that is not a Stick graph.*

Proof. The proof is based on the graph Φ shown in Figure 18. The vertices x and y are the *connectors* of Φ. Let G be a graph that contains an induced Φ and a path p_{xy} from x to y such that there is no adjacency between inner vertices of p_{xy} and the 6-cycle of Φ. Observe that the Stick representation of the 6-cycle is essentially unique. Now it is easy to check that in a Stick representation of G the sticks for the connectors have to be placed like the two blue sticks or like the two red sticks in Figure 18, otherwise the sticks of x and y would be separated by the 6-cycle, whence one of the sticks representing inner vertices of p_{xy} and a stick of the 6-cycle would intersect. Depending on the placement the connectors are of type *inner* (blue) or *outer* (red).

Consider the graph Φ^4 depicted in Figure 19 together with a hook representation of it. Suppose for contradiction that Φ^4 has a Stick representation. It contains four copies $\Phi_1, \ldots, \Phi_4$ of the graph Φ with connectors $x_1, \ldots, x_5$. By our observation above, the connectors of each Φ_i are either of inner or outer type. We claim that for each $i \in \{1, 2, 3\}$, connecters of Φ_i and Φ_{i+1} are of different type. If the type of both connectors of Φ_i and Φ_{i+1} is inner, then such a placement would force extra edges, specifically an edge between the two 6-cycles of Φ_i and Φ_{i+1}. And if both are outer then such a placement would separate x_i and x_{i+2}, see Figure 20 on the left.

It follows that the connector type of the Φ_i's is alternating. In particular, there is $i \in \{1, 2\}$ such that the connectors of $\Phi_i, \Phi_{i+1}, \Phi_{i+2}$ are of type inner–outer–inner in this order. The right-hand side of Figure 20 illustrates how Φ_i and Φ_{i+1} have to be drawn in a Stick representation. Since x_{i+2} is one of the inner type connectors of Φ_{i+2}, there is no chance

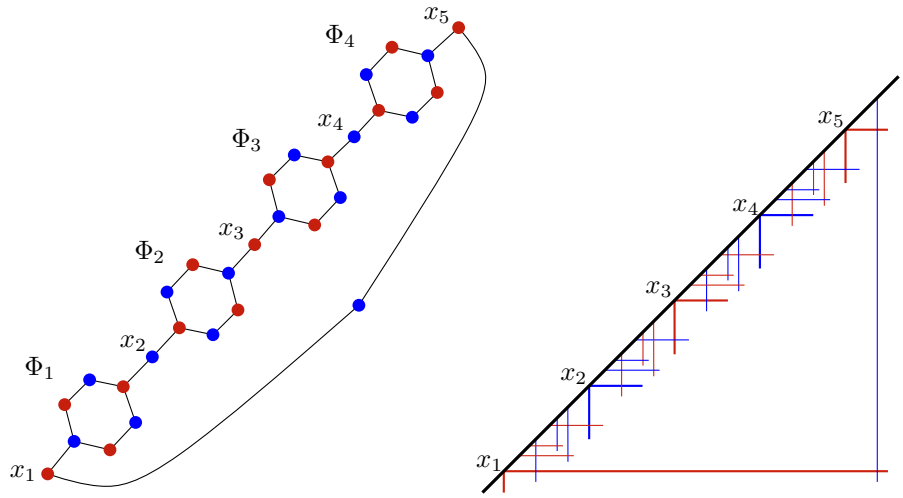

Figure 19: A bipartite hook graph (with hook representation) that is not a Stick graph.

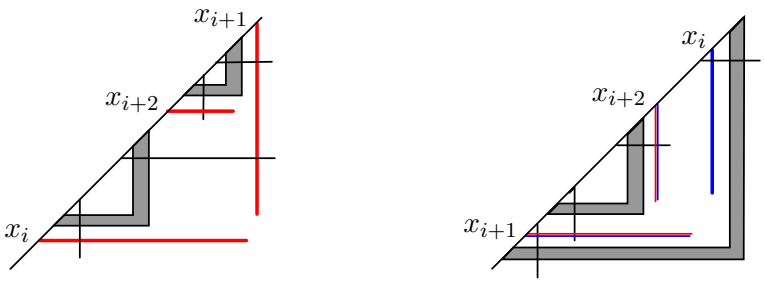

Figure 20: Stick representations of Φ_i and Φ_{i+1} with connecters of type inner–inner (left) and inner–outer (right).

of adding the sticks for Φ_{i+2} to the drawing without intersecting sticks representing Φ_i and Φ_{i+1}. This is a contradiction and hence Φ^4 is not a Stick graph. □

5.3 Stabbability

We proceed to show that

$$\text{SegRay} \not\subset \text{StabGIG} \qquad \text{4-DORG} \not\subset \text{StabGIG}.$$

As an intermediate step we prove that there are GIGs that are not stabbable. Techniques used in the proof will be helpful to show the two seperations.

Proposition 21 *There exists a GIG that is not a StabGIG.*

Proof. Consider a GIG representation of a complete bipartite graph $K_{n,n}$. The GIG representation forms a grid in the plane. Now we add segments such that for every pair of cells in the same row or in the same column there is a segment that has endpoints in both of the cells. Furthermore, those segments can be drawn in such way that a horizontal and a

vertical segment intersect if and only if both intersect a common cell completely, that is, they do not have an endpoint in this cell. Denote the resulting GIG representation by R_n and the corresponding GIG by G_n.

Suppose for contradiction that G_n has a stabbable GIG representation R'_n for all $n \in \mathbb{N}$. By the Erdős-Szekeres theorem for monotone subsequences, for every $k \in \mathbb{N}$ there exists $n \in \mathbb{N}$ such that in R_n there are subsets H and V consisting of k horizontal and k vertical segments that represent vertices of the $K_{n,n}$ in G_n, such that they appear in the same order (up to reflection) as segments in R_n representing the same set of vertices. In R_n those segments induce a subgrid to which we added the blue segments depicted in Figure 21. That is, for each cell c in the subgrid we have a horizontal segment h_c and a vertical one v_c such that h_c and v_c intersect only each other and the segments building the boundary of c.

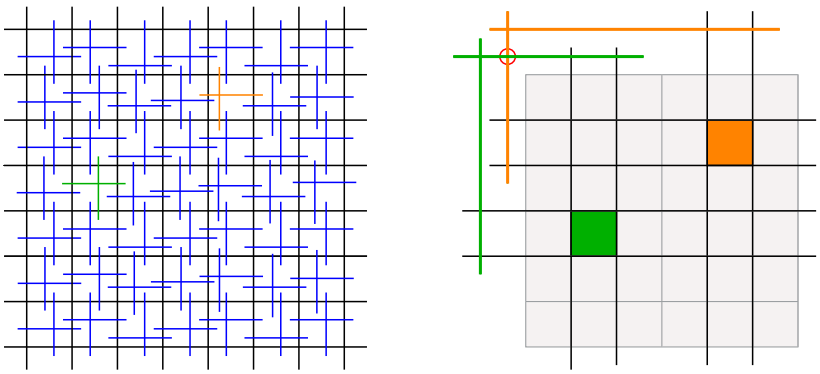

Figure 21: Partial representation of R_n on the left. Replaced cell segments in R'_n on the right.

It is easy to see that this partial representation in R_n is not stabbable if k is large. Since the segments of the subgrid appear in the same order (up to reflection) in R'_n, we only have to consider the placement of cell segments h_c and v_c. We restrict our attention to cells not lying on the boundary of the grid and fix a stabbing line ℓ for R'_n. There are two possibilities for the placement of h_c and v_c in R'_n. One case is that the intersection point p_c of h_c and v_c lies in c or in one of the eight cells surrounding c. Then the segments h_c and v_c can only be stabbed by ℓ if at least one of those eight cells around c is intersected by ℓ. The cells intersected by ℓ in R'_n are only $O(k)$ many, so their neighbouring cells are only $O(k)$ many as well. This shows that $\Omega(k^2)$ intersection points p_c have to lie outside of the grid in R'_n (as depicted in Figure 21 on the right). However, we show that this is possible for only $O(k)$ of them.

If an intersection point lies outside of the grid it is assigned to one quadrant, i.e., p_c lies above or below and left or right of the interior of the grid. Every quadrant contains at most $O(k)$ points p_c: We index each cell by its row and column in the grid so that the bottom- and leftmost cell is $c_{1,1}$. If the intersection points corresponding to cells $c_{u,v}$ and $c_{x,y}$ lie in the upper left quadrant, then $u < x$ implies $y \leq v$. This is illustrated in Figure 21 where it is shown that otherwise the cell segments of the colored cells produce a forbidden intersection. It follows that at most $O(k)$ intersection points of cell segments can lie in one quadrant, and hence $O(k)$ of them lie outside of the grid. We conclude that G_n has no stabbable GIG representation for a sufficiently large n. □

For SegRay graphs we give a similar construction that shows that there are SegRay graphs which do not belong to StabGIG. First we will construct a graph that cannot be stabbed in any SegRay representation.

Lemma 4 *Let R be a SegRay representation of a cycle C with $2n$ vertices. For the vertices in C being represented as rays it holds that their order in C is up to reflection and cyclic permutation equal to the order of the rays representing them in R .*

Proof. Let L be a horizontal line below all horizontal segments in R. Contracting each ray to its intersection point with L yields a planar drawing of a cycle C' with n vertices such that the vertices lie on L and edges are drawn above L. This is also known as a *1-page embedding* of C'. It is easy to see that edges in C' have to connect consecutive vertices on L or the two extremal ones. Now the conclusion of the lemma is straightforward. □

Proposition 22 *There exists a SegRay graph that has no stabbable SegRay representation.*

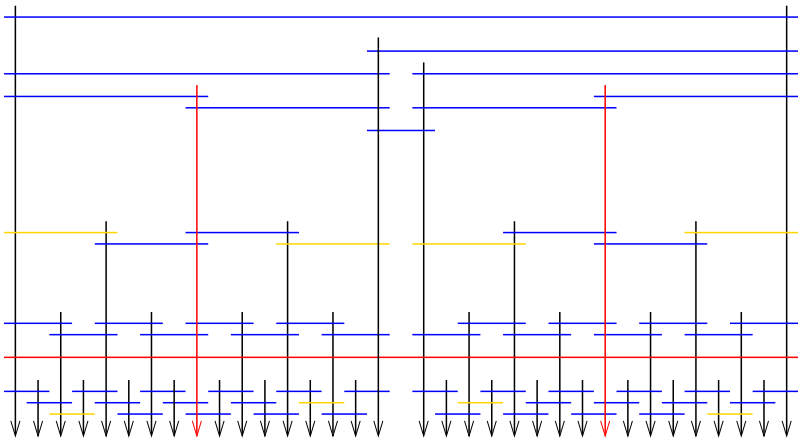

Figure 22: A SegRay graph with no stabbable SegRay representation.

Proof. Consider the graph defined by the SegRay representation R in Figure 22. Let R' be an arbitrary SegRay representation of this graph. The order of the rays in R' is up to reflection and cyclic permutation equal to the one in R by Lemma 4. Hence without loss of generality the rays of the left half in R appear consecutively in R'. Now observe that the two yellow segments below the red segment in the left half of R also have to be below the red segment in R'. Similarly, the two yellow segments above the red segment in R must lie above the red segment in R'. Furthermore, these two yellow segments have to lie below the top of the red vertical ray in R'. It follows that, as in R, the red segment and the red ray seperate the plane into four quadrants in R' such that each quadrant contains exactly one of the considered yellow segments. Any line in the plane can intersect at most three of the quadrants and thus will miss a yellow segment in R'. Therefore, R' is not stabbable and the conlusion follows. □

We add a vertex h to the graph in Figure 22 that is adjacent to all rays. This graph is still a SegRay graph. We call this graph a *bundle* and the set of horizontal segments its *head*.

The bundle is not stabbable in any SegRay representation by the proposition above. This means, in any StabGIG representation of a bundle there is one horizontal segment above the segment representing h and one below. Indeed, otherwise the representation of the bundle can be modified by extending vertical segments to rays in one direction to obtain a stabbed SegRay representation. Using this property of a bundle we can show the following.

Proposition 23 *There exists a SegRay graph that is not a stabbable GIG.*

Proof. Similar to the construction in Proposition 21, consider a SegRay representation of a complete bipartite graph $K_{n,n}$. In this representation we see a grid with cells. We place in each of the cells the head of a bundle as indicated in Figure 23. Now, for each pair of cells in the same row of the grid, add a spanning horizontal segment with endpoints in the given cells. We do it in such a way that the rays of a bundle are intersected by the segment if the head of the bundle lies in a cell between the two given cells.

Denote by R_n the resulting SegRay representation and let H_n be the SegRay graph defined by R_n. Suppose that H_n has a stabbable GIG representation R'_n. As in the proof of Proposition 21, given an integer $k \geq 1$ it follows by the Erdős-Szekeres theorem that for sufficiently large n there is a subgrid of size k in R'_n, where the order of the horizontal and vertical segments is either preserved or reflected with respect to R_n. Assume that it is preserved. Now we restrict our attention to the relevant bundles and horizontal segments of R_n according to the cells of the subgrid. In R_n again this looks like in Figure 23, but this time with respect to the fixed subgrid.

Let us now consider the placement of the bundles and blue segments in R'_n. Given a cell c in the subgrid, let y_c be the horizontal grid segment bounding c from below. By Proposition 22 and its consequences, the bundle lying in cell c contains a horizontal segment that lies above y_c in R'_n. We denote this segment by h_c and let x_c be an arbitrary ray of the bundle intersecting h_c. Consider now the left side of Figure 24 showing a 3×3 box and a ray x of the subgrid that lies strictly to the left of the box in the representation R_n. Let c_1, c_2, c_3 be the three shaded cells. Then we claim that at least one of $h_{c_1}, h_{c_2}, h_{c_3}$ is placed to the right of x in R'_n.

Suppose to the contrary that all lie to the left. If we use the fact that h_{c_i} is above x_{c_i} in R'_n for each $i \in \{1, 2, 3\}$, then it is straightforward to see that $h_{c_1}, h_{c_2}, h_{c_3}, x_{c_1}, x_{c_2}, x_{c_3}$ and the three short blue horizontal segments depicted on the left of Figure 24 have to be placed in R'_n as shown on the right of Figure 24 (segments h_{c_i} are colored purple). But

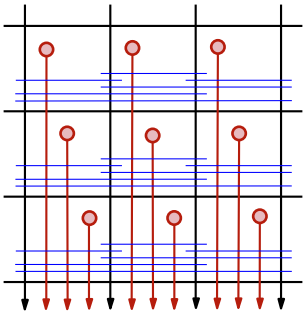

Figure 23: Illustration of a SegRay graph that is not a StabGIG

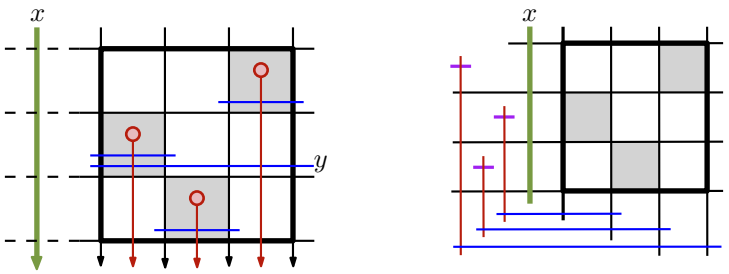

Figure 24: For at least one grey cell c, the purple segment h_c lies to the right of x in R'_n.

then the segment y, which is the long blue one on the left, cannot be added to the partial representation without creating forbidden crossings. This shows our subclaim.

In the next step we consider the green box of the fixed subgrid shown on the left of Figure 25. Using our subclaim we have that each of the three shaded 3×3 boxes contains a cell c such that h_c is placed to the right of x in R'_n. Now we apply the symmetric version of this claim to deduce that one of these three segments also lies to the left of x' in R'_n. We conclude that there is a segment that is strictly contained in the green box in R'_n.

In the final step we consider four copies of the green box that are placed in the fixed subgrid of R_n as shown on the right of Figure 25. Since each copy strictly contains a segment in R'_n, each line in the plane will miss at least one of the four segments. This shows that R'_n is not stabbable for sufficiently large n and completes the proof. □

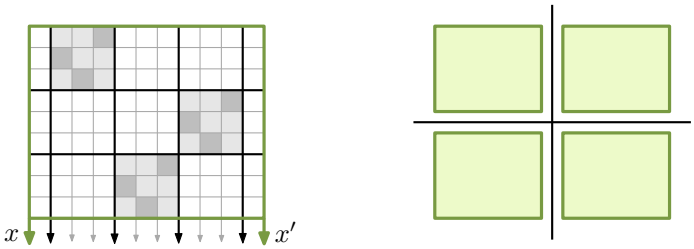

Figure 25: There is a cell c in the green box such that h_c is drawn inside the box in R'_n.

Proposition 24 *There exists a 4-DORG that is not a stabbable in any GIG representation.*

Proof. Since the ideas here are similar to those used for Propositions 22 and 23, we only provide a sketch of this proof. Consider the following construction. Take a 4-DORG representation of a complete bipartite graph $K_{n,n}$. Similarly to previous constructions this yields a grid with cells. For each cell we add four rays starting in this cell, one in each direction and such that a vertical and a horizontal ray intersect if and only if they entirely intersect a common cell. Call this representation R_n and the corresponding intersection graph G_n. We claim that for sufficiently large n there is no stabbable GIG representation of G_n.

Suppose to the contrary that there exists a StabGIG representation R'_n of G_n. Again by applying the Erdős-Szekeres theorem we may assume that there is a large subgrid of size k in R'_n, such that the order of the grid segments in R'_n agrees with the order in R_n (up to reflection).

Given the representation R'_n, we want to partition the cells of the subgrid according to the placement of the four segments representing the rays that start in a given cell of our construction. Note that these four segments intersect in such a way that they enclose a rectangle in R'_n. Therefore, we can distinguish the following cases: the rectangle (1) is contained in a grid cell, (2) it does not intersect a grid cell, (3) it contains some but not all grid cells, and (4) it contains all of the grid cells (see Figure 26 for the cases from left to right). Each of these cases again can be split into at most four natural subcases. For instance, if the rectangle contains some of the grid cells, then it also has to contain a corner of the grid, which gives rise to four subcases.

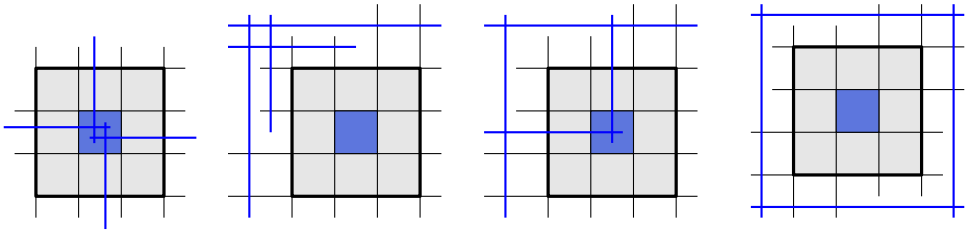

Figure 26: Four different situations for the blue cell and its segments in R'_n

Using similar arguments as in previous proofs of the paper and the assumption that R'_n is stabbed by a line, one can show that each partion class contains at most $O(k)$ cells. Thus, for large enough n and k we get a contradiction since our subgrid has k^2 cells. This observation completes the proof. □

It remains open whether there exists a 3-dimensional GIG that is not stabbable. It is tempting to look for an example that produces again a large grid in every representation (to get non-stabbability), but it turned out that all these examples seem to have dimension 4. We also tried with SegRay graphs satisfying the properties of Lemma 1 since they have dimension 3. However, we didn't succeed with finding such a SegRay that is not stabbable.

6 Conclusion

We have shown that Figure 1 provides the correct inclusion order of the given subclasses of GIG. An overview of the separating examples is given in Table 1.

The notion of order dimension was helpful in particular to exhibit examples that separate classes. As a byproduct we have new insights regarding the interval dimension of vertex-face posets of outerplanar maps (Corollary 2).

Another direction of research regarding these graph classes is recognition. Currently the recognition complexity of some of the graph classes remains open, see the table below. We hope that our results help bringing these open problems closer to a solution.

Class	recognition complexity	reference
GIG	NP-complete	[21]
UGIG	NP-complete	[22]
3-dim BipG	NP-complete	[14]
3-dim GIG	Open	
StabGIG	Open	
SegRay	Open	
BipHook	Open	
Stick	Open	
4-DORG	Open	
3-DORG	Open	
2-DORG	Polynomial	[25],[9]
bipartite permutation	Polynomial	[11]

References

[1] E. Ackerman, G. Barequet, and R. Y. Pinter, *On the number of rectangulations of a planar point set*, Journal of Combinatorial Theory, Series A, 113 (2006), 1072–1091.

[2] S. Cabello, J. Cardinal, and S. Langerman, *The clique problem in ray intersection graphs*, Discrete & computational geometry, 50 (2013), 771–783.

[3] D. Catanzaro, S. Chaplick, S. Felsner, B. Halldórsson, M. Halldórsson, T. Hixon, and J. Stacho, *Max-point-tolerance graphs*, Discrete Applied Mathematics, to appear (2015).

[4] T. M. Chan and E. Grant, *Exact algorithms and APX-hardness results for geometric packing and covering problems*, Computational Geometry, 47 (2014), 112–124.

[5] S. Chaplick, E. Cohen, and G. Morgenstern, *Stabbing polygonal chains with rays is hard to approximate*, in Proceedings of the 25th Canadian Conference on Computational Geometry, 2013.

[6] S. Chaplick, P. Hell, Y. Otachi, T. Saitoh, and R. Uehara, *Intersection dimension of bipartite graphs*, in TAMC, vol. 8402 of LNCS, Springer, 2014, 323–340.

[7] V. Chepoi and S. Felsner, *Approximating hitting sets of axis-parallel rectangles intersecting a monotone curve*, Computational Geometry, 46 (2013), 1036–1041.

[8] F. J. Cobos, J. C. Dana, F. Hurtado, A. Márquez, and F. Mateos, *On a visibility representation of graphs*, in Graph Drawing, vol. 1027 of LNCS, 1996, 152–161.

[9] O. Cogis, *On the Ferrers dimension of a digraph*, Discrete Mathematics, 38 (1982), 47–52.

[10] J. R. Correa, L. Feuilloley, and J. Soto, *Independent and hitting sets of rectangles intersecting a diagonal line*, in LATIN, vol. 8392 of LNCS, 2014, 35–46.

[11] B. Dushnik and E. Miller, *Partially ordered sets*, American Journal of Mathematics, 63 (1941), 600–610.

[12] S. Felsner, *Exploiting air-pressure to map floorplans on point sets*, in Graph Drawing, vol. 8242 of LNCS, 2013, 196–207.

[13] S. Felsner, *The order dimension of planar maps revisited*, SIAM Journal on Discrete Mathematics, 28 (2014), 1093–1101.

[14] S. Felsner, I. Mustaţă, and M. Pergel, *The complexity of the partial order dimension problem – closing the gap*, arXiv:1501.01147, (2015).

[15] S. Felsner and J. Nilsson, *On the order dimension of outerplanar maps*, Order, 28 (2011), 415–435.

[16] S. Felsner and W. T. Trotter, *Posets and planar graphs*, Journal of Graph Theory, 49 (2005), 273–284.

[17] B. V. Halldórsson, D. Aguiar, R. Tarpine, and S. Istrail, *The clark phaseable sample size problem: Long-range phasing and loss of heterozygosity in GWAS*, Journal of Computational Biology, 18 (2011), 323–333.

[18] T. Hixon, *Hook graphs and more: some contributions to geometric graph theory*, master's thesis, TU Berlin, 2013.

[19] M. J. Katz, J. S. Mitchell, and Y. Nir, *Orthogonal segment stabbing*, Computational Geometry, 30 (2005), 197–205.

[20] A. V. Kostochka and J. Nešetřil, *Coloring relatives of intervals on the plane, i: chromatic number versus girth*, European Journal of Combinatorics, 19 (1998), 103–110.

[21] J. Kratochvíl, *A special planar satisfiability problem and a consequence of its NP-completeness*, Discrete Applied Mathematics, 52 (1994), 233–252.

[22] I. Mustaţă and M. Pergel, *Unit grid intersection graphs: Recognition and properties*, arXiv:1306.1855, (2013).

[23] W. Schnyder, *Planar graphs and poset dimension*, Order, 5 (1989), 323–343.

[24] A. M. S. Shrestha, A. Takaoka, and T. Satoshi, *On two problems of nano-PLA design*, IEICE transactions on information and systems, 94 (2011), 35–41.

[25] A. M. S. Shrestha, S. Tayu, and S. Ueno, *On orthogonal ray graphs*, Discrete Applied Mathematics, 158 (2010), 1650–1659.

[26] F. W. Sinden, *Topology of thin film RC circuits*, Bell System Technical Journal, 45 (1966), 1639–1662.

[27] M. Soto and C. Thraves, *p-box: A new graph model*, Discrete Mathematics and Theoretical Computer Science, 17 (2015). 18 pages.

[28] R. Tamassia and I. G. Tollis, *A unified approach to visibility representations of planar graphs*, Discrete & Computational Geometry, 1 (1986), 321–341.

[29] C. Telha and J. Soto, *Jump number of two-directional orthogonal ray graphs*, in IPCO, vol. 6655 of LNCS, 2011, 389–403.

[30] W. T. Trotter, *Combinatorics and Partially Ordered Sets: Dimension Theory*, Johns Hopkins Series in the Mathematical Sciences, The Johns Hopkins University Press, 1992.

[31] W. T. Trotter, Jr., J. I. Moore, Jr., and D. P. Sumner, *The dimension of a comparability graph*, Proc. Amer. Math. Soc., 60 (1976), 35–38 (1977).

[32] S. K. Wismath, *Characterizing bar line-of-sight graphs*, in Proceedings of the annual symposium on computational geometry, ACM, 1985, 147–152.